The investigation of locus coeruleus noradrenergic neuronal circuitry change and neuronal plasticity after permanent focal cerebral ischemia in mice using genetic tracing method.

Hyun Jung Kim

Department of Medical Science

The Graduate School, Yonsei University

The investigation of locus coeruleus noradrenergic neuronal circuitry change and neuronal plasticity after permanent focal cerebral ischemia in mice using genetic tracing method.

Directed by Professor Byung In Lee

The Master's Thesis
Submitted to the Department of Medical Science,
The Graduate School of Yonsei University
In partial fulfillment of the requirements
For the degree of Master of Medical Science

Hyun Jung Kim

December 2006

This certifies that the Master's Thesis

of Hyun Jung Kim is approved.

_____

Thesis Supervisor: Byung In Lee

_____

Young Buhm Huh

_____

Jong Eun Lee

The Graduate School
Yonsei University

December 2006

TABLE OF CONTENTS

LIST OF FIGURES

LIST OF TABLES

ABSTRACT

The investigation of locus coeruleus noradrenergic neuronal circuitry change and neuronal plasticity after permanent focal cerebral ischemia in mice using genetic tracing method.

Hyun Jung Kim

Department of Medical Science
The Graduate School, Yonsei University

(Directed by Professor Byung In Lee)

Identifying neuronal network is essential for the investigation of various brain functions. For visualization of selective and functional neural circuitry, a novel genetic strategy employing wheat germ agglutinin (WGA) cDNA under the control of cell-specific promoter elements has been introduced as a powerful tool. Dysfunction of noradrenergic system has been reported in various neurological disorders such as Alzheimer's disease, Parkinson disease, or acute ischemic stroke, etc. However, exact locations or extent of noradrenergic circuitry damage and its functional implications are remaining to be elucidated. In this study, a novel genetic tracing method, the combination of noradrenergic-specific promoter and WGA, was used to visualize noradrenergic neuronal circuitry in mice, which were followed by further investigations aiming at the establishment of

relationships between alterations of noradrenergic neuronal circuitry and functional recovery in a permanent focal cerebral ischemia (pFCI) model.

Adult male C57BL/6 mice were subjected to pFCI by intraluminal suture occlusion of middle cerebral artery (MCAO) under the monitoring of regional cerebral blood flow (CBF) and blood pressure. The recombinant adenoviral vector introducing WGA cDNA under the control of noradrenergic neuron-specific PRS promoter was injected in the ipsilateral locus coeruleus of ischemic brain. Through the immunohistochemistry and *in situ* hybridization, the expression of WGA protein and mRNA were examined in pFCI induced mice to compare with control. 5-bromo-2'-deoxyuridine (BrdU) labeling was also performed to search newly forming neurons and their reorganization processes. The measurement of blood pressure, body temperature, body weight, and behavioral tests assessing anxiety were also performed.

In non-injured brain, intense WGA immunoreactivity was detected in various brain regions including pontine reticular nucleus, thalamic nucleus, lateral hypothalamic area, amygdala, and olfactory bulb. This study also demonstrated that the physiological dysfunctions resulting from structural damages involving thalamic and hypothalamic lesions were recovered by subquent reorganization of noradrenergic system after ischemic injury, which was consistent with the hypothesis of "structural neural plasticity being responsible for functional recovery" in noradrenergic system.

Key Words: Cerebral ischemia, focal; Norepinephrine; Agglutinins, Wheat Germ; Vector, Genetic; Plasticity, Neuronal

The investigation of locus coelureus noradrenergic neuronal circuitry change and neuronal plasticity after permanent focal cerebral ischemia in mice using genetic tracing method.

Hyun Jung Kim

Department of Medical Science

The Graduate School, Yonsei University

(Directed by Professor Byung In Lee)

I. INTRODUCTION

Cardiac complications including sudden death, arrhythmia or myocardial damage are frequent during recovery phase after stroke.[1] In addition, plasma noradrenaline (NA) levels are often elevated,[2-4] which may be responsible for increased serum cardiac enzyme, tachycardia and high cardiac output, and high blood pressure.[5, 6,7] Experimentally, plasma level of NA was significantly elevated compared to that of preocclusion condition after permanent occlusion of left MCA in cat.[8] Dysfunction of the noradrenergic system is a frequent feature in various neurodegenerative disorders such as Alzheimer's disease, Parkinson disease, multisystem atrophy as well as in acute ischemic stroke. Defects in the noradrenergic system have also been implicated in many psychiatric disorders manifesting

abnormal social behavior, attention deficit, hyperactivity, anxiety, and depression. NA is the neurotransmitter being implicated in many of these disorders and has been found to affect social behavior in both humans and animals.[9] Therefore, investigating alterations of NA systems in stroke may provide clues to understand its symptomology, clinical courses, and adequate management.[10, 11]

Locations and size of stroke may be related to different characteristics of autonomic dysfunction.[12] The most important control sites of autonomic function are found to be the insular cortex, amygdala, and lateral hypothalamus[5] and, among these, insular cortex and amygdala are supplied by seem MCA and play a crucial role in cardiovascular regulation.[13, 14] Brain ischemia induces both pathological synaptic plasticity causing delayed neuronal

Abbreviations

A5	A5 noradrenaline cells	lo	lateral olfactory tract
aca	anterior commissure, anterior part	LPAG	lateral periaqueductal gray
aci	anterior commissure, intrabulbar part	LPB	lateral parabrachial nucleus
Arc	arcuate hypothalamic nucleus	LSI	lateral septal nucleus, intermediate part
BL	basolateral amygdaloid nucleus	Me5	mesencephalic trigeminal nucleus
bsc	brachium of the superior colliculus	mlf	medial longitudinal fasciculus
cc	corpus callosum	Mo5	motor trigeminal nucleus
cg	cingulum	MPB	medial parabrachial nucleus
Cg2	cingulate cortex, area 2	Op	optic nerve layer of the superior colliculus
CIC	central nucleus of the inferior colliculus	opt	optic tract
cp	cerebral peduncle, basal part	P5	peritrigeminal zone
CPu	caudate putamen	PCRt	parvicellular reticular nucleus
DG	dentate gyrus	Pir	piriform cortex
DLPAG	dorsolateral periaqueductal gray	Pn	pontine nuclei
DpMe	deep mesencephalic nucleus	Pr5	principal sensory trigeminal nucleus
DRV	dorsal raphe nucleus, ventral part	RSA	retrosplenial agranular cortex
f	fornix	RSG	retrosplenial granular cortex
hf	hippocampal fissure	Rt	reticular thalamic nucleus
ic	internal capsule	sm	stria medullaris of the thalamus
InG	intermediate gray layer of the superior colliculus	SNL	substantia nigra, lateral part
InWh	intermediate white layer of the superior colliculus	SuG	superficial gray layer of the superior colliculus
La	lateral amygdaloid nucleus	VP	ventral pallidum
LC	locus coeruleus	VPL	ventral posterolateral thalamic nucleus
LH	lateral hypothalamic area	VPM	ventral posteromedial thalamic nucleus
LHb	lateral habenular nucleus		

death and induce physiological plasticity, leading structural reorganization resulting in functional recovery.[15, 16] Thus, it has been suggested that ischemia may promote activity-dependent plasticity essential for the recovery of neurological deficits seen in many patients after a stroke.[17-19]

The wiring patterns of various neuronal populations connected by specific synaptic connections are the basis of functional logic for information processing employed by brain. To accurately identify patterns of neuronal connectivity, various neuroanatomical tracers have been used for labeling axons and dendrites of specific neurons projecting to their synaptic partner neurons.[20-22]

Plant lectins have been widely used as highly sensitive tracers in anatomical studies for mapping central neural pathways.[23, 24] Among various plant lectins, WGA has been extensively studied and proved to be most efficiently transferred by projecting neurons.[25, 26] The WGA protein injection method had been used to visualize optic pathways[27, 28] in monkeys, olfactory systems[24, 29] in rodents, common afferent projections to locus coelureus (LC)[30] in rat, and connections of the A5 noradrenergic cell group[31] in rat. However, the potential problem of direct injection method is hampered by its neuronal non-specificity causing all neurons located at the injection site to take up WGA protein resulting in labeling of unrelated pathways.[21, 22] Recently, a novel genetic strategy employing cDNA for WGA as a transgene under the control of specific promoter elements, was introduced in neural tracing study. Studies using the genetic method were successfully conducted in transgenic mice to visualize optic pathways[32], sensory map in olfactory cortex[33], cerebellar efferent pathway[20] and taste neuronal circuitries for bitter and sweet[34]. The use of WGA-

expressing adenoviral vector system for visualization of neural circuitries were further expanded to a wide range of hosts, which were transferred genes in time- and place-specific manners, including the tracing of olfactory pathway in mouse[22] and the remodeling of intraspinal or cortical circuitries with functional recovery after spinal cord injury[21, 35].

This study was conducted to visualize noradrenergic neuronal circuitry using a novel genetic tracing method and to investigate the temporal relationships between the alteration of noradrenergic circuitries and functional recovery after pFCI in mice.

II. MATERIALS AND METHODS

1. Focal cerebral ischemia

Adult male C57BL/6 mice (22-27g; Orient Co., Kyonggi-do, South Korea) were housed in a 12h light/dark cycle and permitted food and water. These mice were anesthetized by inhalation of isoflurane in N_2O/O_2 (70:30%) and subjected to pFCI by MCA blockade with a 5.0 surgical monofilament nylon suture. At the end of surgery, the nylon suture was tightly fixed at the final position with a silk suture. A Laser Doppler flowmeter (transonic system Inc., New York, USA) with the probe placed directly on the skull surface over the territory of the MCA (1mm posterior and 5mm lateral to bregma), measured regional CBF before and after occlusion and immediately before sacrifice. Cannulation of a femoral artery allowed the monitoring of blood pressure with Pressure Transducer (Harvard Apparatus, Inc., Holliston, MA, USA). All procedures were approved by the animal care committee at Yonsei University medical college.

2. Infarct size measurement

Seven serial 40 μm thick slice coronal sections from each brain were cut at 800 μm intervals beginning at 2mm from the front using a cryostat. Each slice was stained with cresyl violet. Infarct sizes were expressed as contralateral hemisphere (mm^3) minus undamaged ipsilateral hemisphere (mm^3) to correct for brain edema.[36]

3. Recombinant adenoviral construction and viral infection

The procedure for generation of recombinant adenoviruses was described previously.[38] The PRS-WGA adenovirus was friendly gifted from Dr. Huh, Kyunghee University. A gene cassette containing the WGA gene down stream of the PRS2x8 promoter was inserted into the pAdTrack plasmid and finally into the pAdEasy1. Recombinant adenoviral DNA was cut with Pac1 and transfected into HEK293 cells using Lipofectamine (Invitrogen, California, USA). Viruses were harvested 5days after transfection from the transfected HEK293 cells and amplified on dishes. The viral particles were purified by cesium chloride density gradient ultracentrifugation, dialyzed, and tittered.

Animals were anesthetized and placed in a stereotaxic instrument. After incision of the skin, a small burr hole was made directly at coordinates of LC (5.4 mm posterior, 1.0 mm lateral, and 3.8 mm deep to bregma) and the viral vector was unilaterally injected into the LC of ischemic hemisphere using a Hamilton syringe (Hamilton Co., Nevada, USA). A single injection of 0.2~0.3$\mu\ell$ of the concentrated adenovirus suspension (about 2×10^{13} cfu/ml) was used in this study. The scalp was then sutured, and, after the mouse was returned to standard housing. After 2 days of virus injection, mice were perfused with 4% formaldehyde and the brains were removed for histological analysis

4. Immunohistochemistry

Fixed mouse brains were cut with a cryostat to obtain 40 μm sections, respectively. The sections were pretreated for 20 min with 1% H_2O_2 in PBS containing 0.3% Triton X-100 for inactivation of endogenous peroxidase activity and permeabilization of cells. The

sections were then incubated for 30 min with 5% normal rabbit serum in PBS to block nonspecific protein-binding sites and incubated with anti-WGA polyclonal antibody (1:2000, Vector Laboratory, Burlingame, CA) and anti-tyrosine hydroxylase (TH) polyclonal antibody (1:500, Chemicon, Temecula, CA) in PBS containing 0.3% Triton X-100 with 2% normal rabbit serum overnight at 4°C and for 2 h at room-temperature. After washing, the sections were incubated with biotin-labeled anti-goat IgG (1:200, Vector Laboratory) followed by Vectastatin ABC elite kit (Vector Laboratory), TSA kit (Perkin Almer, Boston, USA) and Vectastatin ABC elite kit again. Signals were visualized with Ni^{2+}-intensified diaminobenzidine/peroxide reaction kit (Vector Laboratory). Specimens were observed with a microscope and computerized digital camera system (Olympus, Tokyo, Japan: Provis), and an image analysis system and program (Adobe Photoshop, San Jose, CA). Evaluation of WGA immunoreactivity levels in various regions of interest was performed as a blind experiment by comparing the stained sections of all mice perfused at different time points in accordance with following criteria[22]: very high (+++), high (++), weak but significant (+), faint (±), or no expression (-) of the WGA transgene product.

5. *In situ* Hybridization

All steps of in situ hybridization were performed essentially as described.[33] Sections of formaldehyde-fixed mouse tissues were treated with proteinase K (10 μg/ml at 25°C for 20 min), acetylated, dehydrated, and air dried. The sections were hybridized for 2hr at 56°C in a humidified chamber with DIG-labeled cRNA probe. After hybridization, the sections were washed in 5× SSC, treated with 50% formamide and RNase A (10 μg/ml at 37°C for

30 min), washed in 2× and 0.2× SSC progressively. The sections were then washed in PBS and incubated with anti-DIG polyclonal antibody (1:2000, Roche Diagnostics GmbH, Penzberg, Germany) in PBS with 5% normal rabbit serum. The sections were detected with avidin-Texas Red (Vector Laboratory). The labeled sections were analyzed with a microscope and computerized digital camera system under fluorescent light (Olympus).

6. BrdU labeling and tissue processing

Cell proliferation was measured by the incorporation of the thymidine analogue 5'-bromo-2-deoxyuridine (BrdU) that is incorporated into the DNA of dividing cells in immunohistochemically detectable quantities during the S phase of cell division. After pFCI, the animals were injected intraperitoneally with BrdU (Roche) (50 mg/kg at a concentration of 10 mg/mL in 0.9% NaCl) and all animals were then sacrificed 4 hours after the BrdU injection.

For immunohistochemical detection of incorporated BrdU, double-stranded DNA was denatured to a single-stranded form suitable for immunohistochemical detection on sections. Sections were incubated in 50% formamide in standard sodium citrate at 65℃ for 2 hr, and treated further with 2 M HCl at 35°C for 30 min. After being rinsed for 10 min at room temperature in 0.1 M boric acid, the sections were washed with PBS and then incubated with 0.03% H2O2 in methanol for 5 min. After having been blocked with the MOM immunodetection kit (Vector Laboratory) according to the standard protocol, the sections were incubated with a primary antibody against BrdU (1:1,000, Roche Diagnostics) at room temperature for 30 minutes, washed with PBS, reacted with a

biotinylated secondary antibody against mouse IgG (1:200) for 10 min at room temperature, and then reacted with streptavidin-biotin-peroxidase complexes for 1hr at room temperature. The peroxidase reaction was visualized by incubation of the sections in diaminobenzidine/hydrogen peroxide solution.

7. Behavioral assessment

The elevated plus maze was comprised of two open arms (25 cm × 5 cm) and two closed arms (25 cm × 5 cm × 5 cm) that extended from a central platform (5 cm × 5 cm). Mice were placed individually in the center square facing an open arm and allowed to explore the maze for 1 min. An arm entry was counted only when all four paws were inside the arm. Measures scored included: (1) time spent in open arms, (2) time spent in closed arms, (3) number of open arm entries, (4) number of closed arm entries.

8. Data analysis

The dada were expressed as mean ± S.D. The statistical comparisons were performed by unpaired t-test and one-way ANOVA (StatView, SAS Institute, Inc., Cary, NC, USA). The significance between the groups was assigned at $p^* < 0.05$ and $p^{**} < 0.001$.

III. RESULTS

1. Adenovirus-mediated WGA expression in LC

In this study, mice were observed at 2 days after viral infection and there was no evidence of cell loss or tissue damage due to the viral infection in LC. In addition, all of the experimental animals that recovered after the infection remained healthy until being sacrificed without exhibiting any behavioral abnormalities.

Figure 1A show an adenoviral construct containing WGA gene under control of the eight copies of PRS promoter. All viruses contained the green fluorescent protein (GFP) gene under the control of the CMV promoter, allowing direct observation of viral delivery to the target sites. After injection of PRS-WGA adenovirus to the LC, localization of GFP expression, WGA protein and mRNA was examined on adjacent coronal sections. Colocalization of GFP, TH, and WGA in adjacent sections clearly demonstrated that recombinant adenoviral particles were precisely delivered to TH-expressing NA neuron in the LC and WGA protein was endogenously synthesized in NA neuron of LC (Figure 1B). In situ hybridization analysis revealed that WGA mRNA was expressed exclusively in LC while no mRNA signal were detected in other sites of brain (Figure 1C).

2. Transsynaptic transfer of WGA in noradrenergic neurons of non-injured mice

In sagittal sections of non-injured brain, intense WGA immunoreactivity was detected in the pontine reticular nucleus, motor and sensory trigeminal nucleus, thalamic nucleus, lateral hypothalamic area, deep mesencephalic nucleus, superior colliculus, caudate

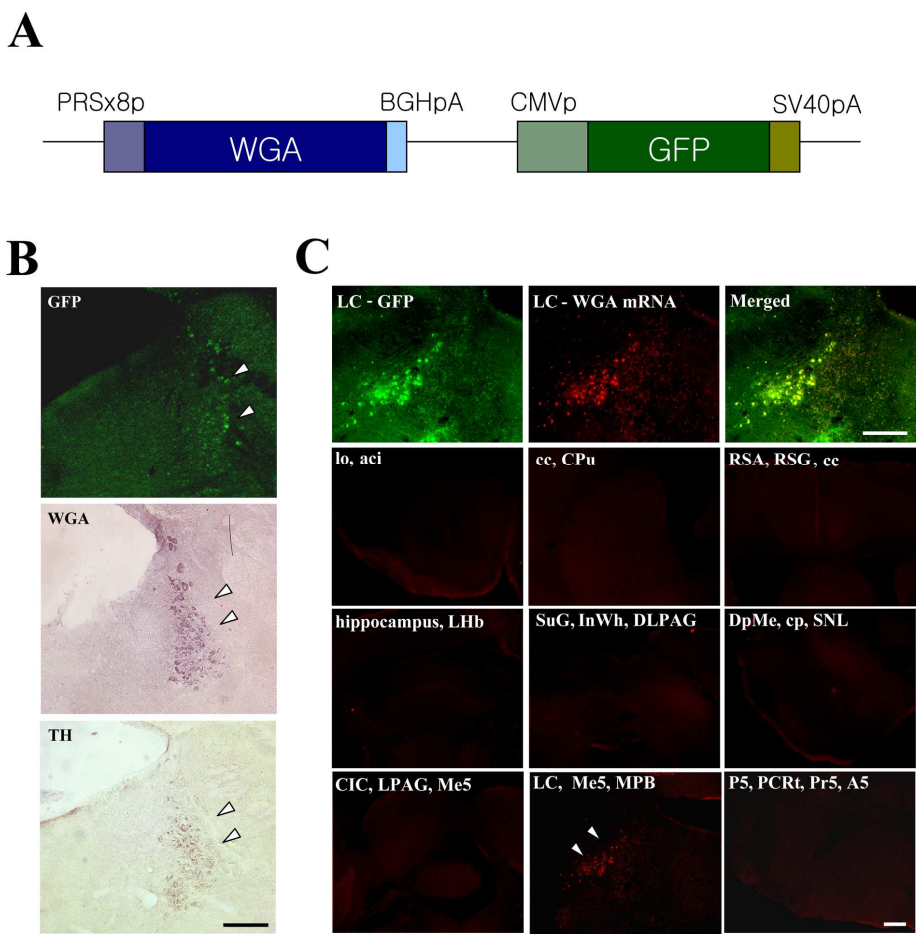

Figure 1. Generation and expression of the PRS-WGA adenovirus. (A) Schematic diagram indicating the structure of the transgene. (B) Adenoviral GFP expression and WGA immunoreactivity were colocalized in TH-positive noradrenergic cell in WGA-adenovirus injected LC. (C) In situ hybridization analysis revealed that WGA mRNA was expressed restrictedly in LC neurons. In contrast, no mRNA signal could be detected in other areas of the brain. Scale bar = 500㎛.

A

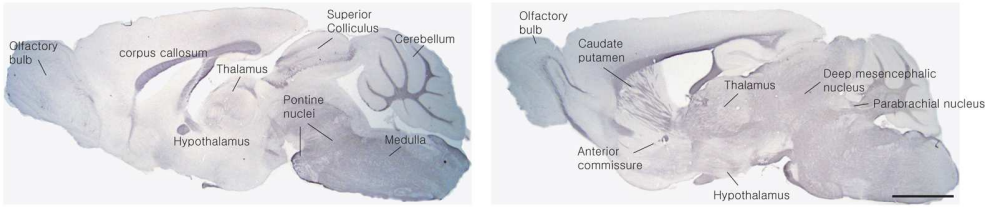

B

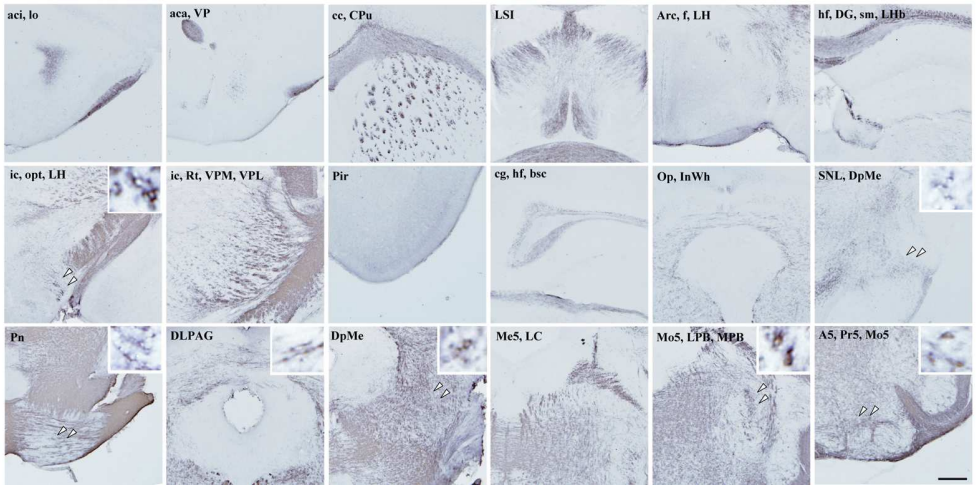

Figure 2. WGA immunoreactivity in non-injured mouse brain. After 2days of PRS-WGA adenovirus injection in LC, LC-originated WGA protein was detected in neurons of several noradrenergic nuclei and other areas. (A) Sagittal sections, scale bar = 5mm and (B) Coronal sections, scale bar = 1mm.

putamen, corpus callosum, anterior commissure, and olfactory bulb (Figure 2A). WGA immunoreactivity was also observed in parabrachial nucleus, A5 noradrenergic cells, substantia nigra, lateral habenular nucleus, hippocampus, optic tract, and piriform cortex in coronal sections (Figure 2B). In the higher magnification field, perikarya were detected in mesencephalic, principal sensory and motor trigeminal nucleus, A5 noradrenergic cells, pontine reticular nucleus, deep mesencephalic nucleus, substantia nigra lateralis, and lateral hypothalamic area (small box in Figure 2B).

3. Ischemic brain damage after MCA occlusion

Infarct volume and size measurements from 7 sections of brain (Figure 3A, B) indicated a significant reduction in lesion size at 8 months after permanent MCA occlusion. Doppler monitoring showed the relative CBF was reduced to 22.6 % ± 5.3 % of pre-occlusion values within 5 minutes of induction of MCAO in mice (Fig. 3C).

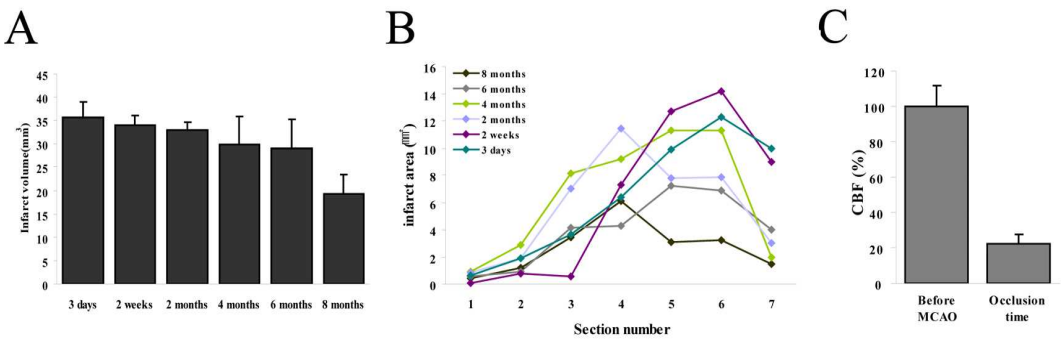

Figure 3. Infarct area measurement and regional CBF. (A), (B) Lesion volumes and areas had time-dependently reduced after permanent focal cerebral ischemic injury. (C) Relative CBF was reduced immediately and continued after pFCI.

4. Anatomical changes of noradrenergic circuit after permanent ischemic damage

In acute stage (for first 1 month) after pFCI, noradrenergic circuits containing thalamic area, lateral hypothalamic area, cortex, and hippocampus were destroyed with severe infarction (data not shown). In long-term observation (Figure 4, Table 1), WGA immunoreactivity was not detected in thalamic nucleus, lateral hypothalamic area, hippocampus, amygdaloid nucleus, superior colliculus in ipsilateral hemisphere before 6 months of pFCI onset. In contrast, a very strong WGA immunoreactivity was observed in the contralateral side, undamaged areas of ipsilateral side, and newly recognized in ipsilateral retrosplenial agranular cortex, caudate putamen, mammilothalamic tract, hippocampal fissure, lateral subventricular zone (SVZ), and lateral hypothalamic area. These features indicated that damaged noradrenergic circuits were partly reorganized over time in the area of previous lesion. Especially, hippocampus, thalamic nucleus, lateral hypothalamic area and amygdaloid nucleus were almost completely reorganized at 8 months after pFCI, while WGA immunoreactivity was not detected internal capsule, fornix, piriform cortex, and superior colliculus. More details were showed in Table 1.

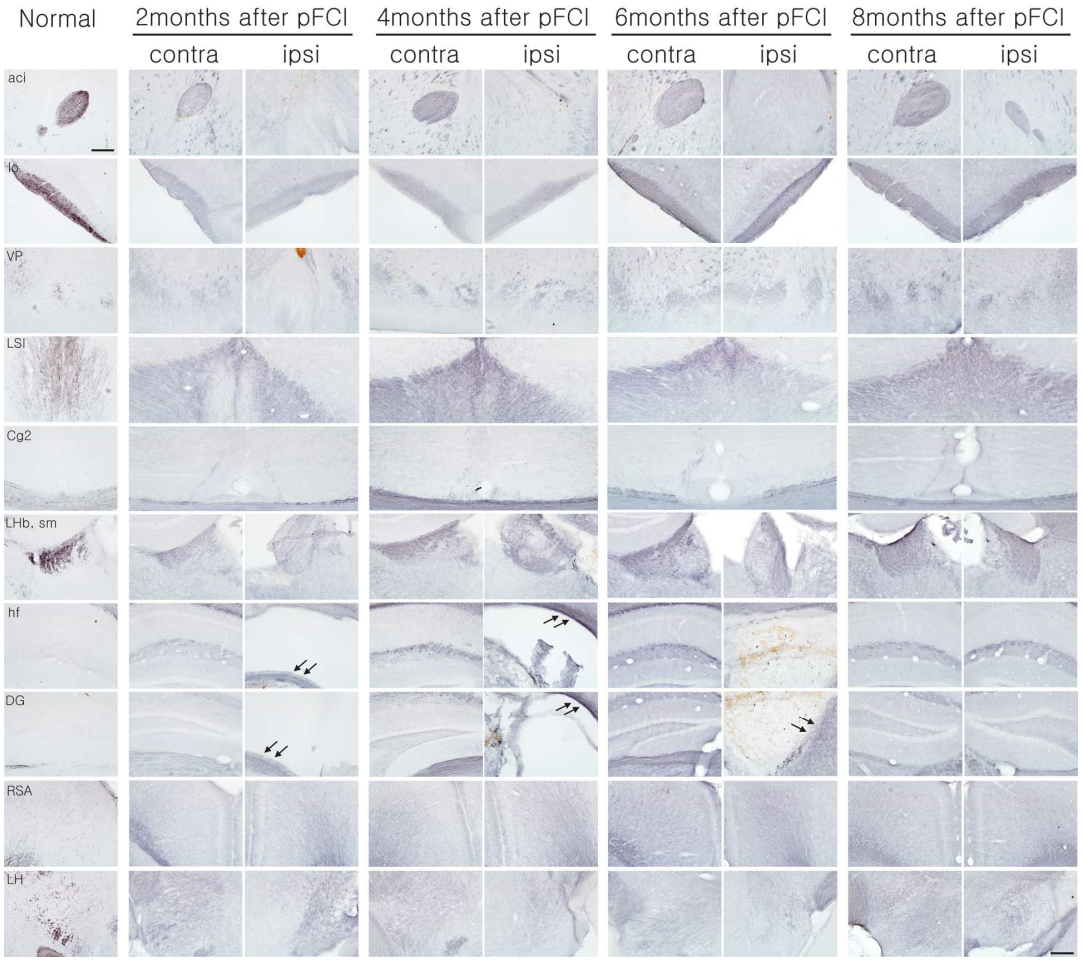

Figure 4. (Continued)

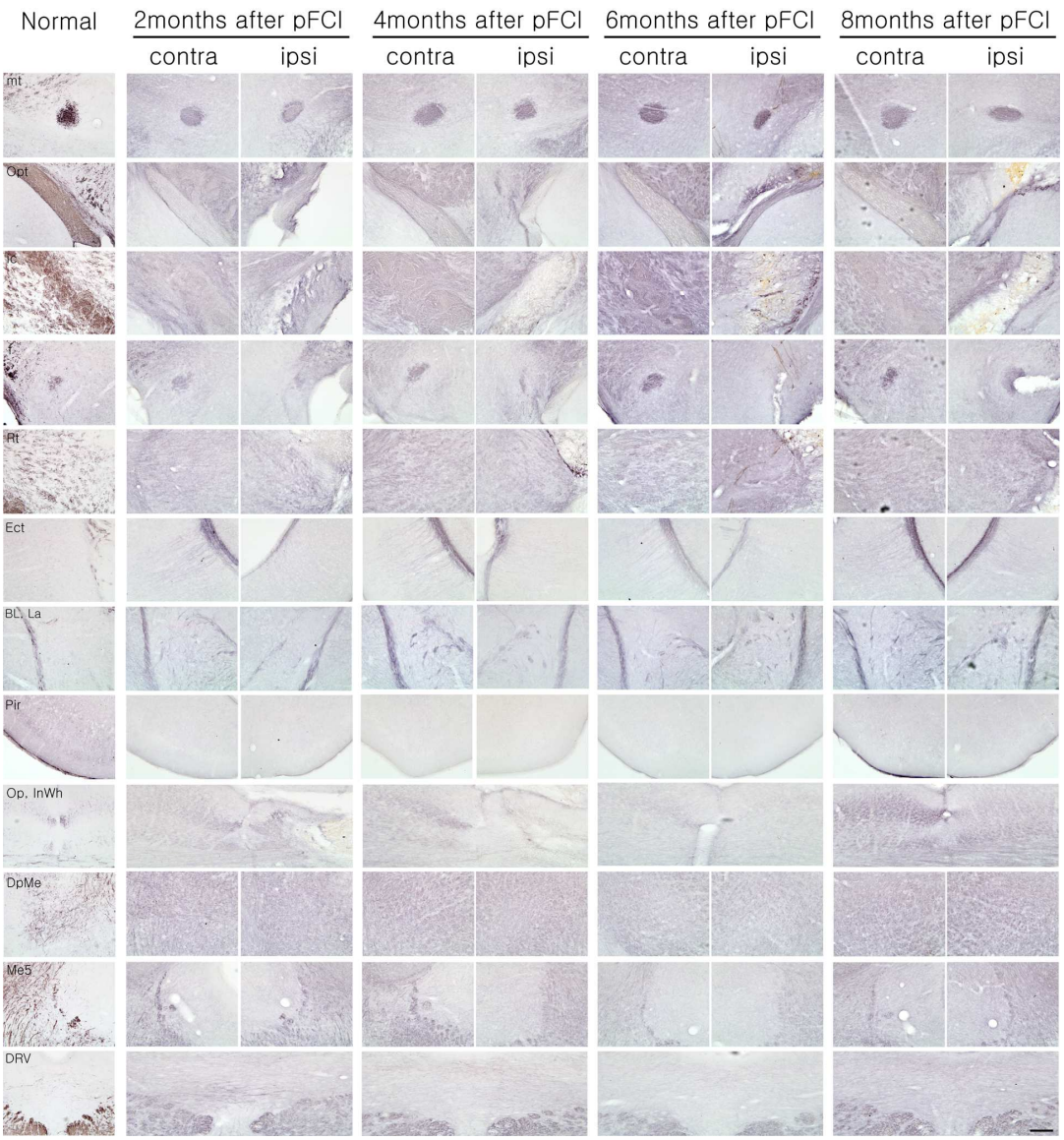

Figure 4. WGA immunoreactivity after pFCI. The WGA positive-neurons were not detected in lesion sites within 6 months after ischemic injury, whereas reorganized WGA positive cells were newly found in several lesioned sites except for piriform cortex, internal capsule and superior colliculus at 8 months after pFCI. Scale bar = 500㎛.

Table 1. WGA expression in whole brain 2 days after PRS-WGA adenovirus injection in pFCI induced mice

WGA immune-reactive site	Normal	2month		4month		6month		8month	
		contra	ipsi	contra	ipsi	contra	ipsi	contra	ipsi
aci	++	++	-	++	-	++	-	++	+
lo	++	+	+	+	+	++	++	++	++
VP	++	++	+	++	++	++	++	++	++
LSI	++	++	+	++	+	++	+	++	++
Cg2	-	+	+	+	-	+	-	+	+
LHb, sm	++	++	+	++	+	++	+	++	++
hf	±	+	-	++	-	++	-	++	++
DG	±	+	-	++	-	++	-	++	++
RSA	++	++	+++	++	++	++	++	++	++
LH	++	++	+	++	±	++	±	++	++
mt	+++	++	++	++	++	++	+	++	++
Opt	+++	++	-	++	-	++	+	++	+
ic	+++	++	+	++	-	++	-	++	-
f	++	++	+	++	±	++	-	++	±
Rt	++	++	+	++	±	++	+	++	++
Ect	±	++	-	++	−	++	+	++	+
Pir	++	-	-	-	-	-	-	±	±
BL, La	±	++	±	++	+	++	++	++	++
Op	+	+	-	++	-	++	-	+++	-
InWh	±	+	-	+	-	±	-	++	++
DpMe	++	++	++	++	+	++	+	++	++
Me5	++	++	++	++	-	+	-	++	++
DRV	-	++	-	+	-	-	-	-	-

+++, very high; ++, high; +, weak; ±, faint; -, no expression.

5. BrdU labeling

Widespread BrdU immunopositive cells were observed in the postischemic corpus callosum, thalamic areas, hypothalamic areas, and hippocampus ipsilateral to the ischemic infarct at 1 month and 6months after pFCI (Figure 5). BrdU-positive cells were more frequently observed in the ipsilateral SVZ than the contralateral side. At 1month after pFCI, many BrdU immunopositive cells were detected in the lesioned thalamus and hypothalamus, and many BrdU positive fusiform-shaped nuclei suggesting migrating cells were also observed in SVZ and corpus callosum of both hemispheres. A 6 months after pFCI, the incidence of BrdU positive cells in the ipsilateral thalamus and hypothalamus was significantly diminished compared to that of 1month after pFCI. No BrdU immunolabeling was detected in contralateral side, except for SVZ and corpus callosum.

6. Neurological outcome and physiological parameters

The mean arterial blood pressure (MABP) increased gradually to peak at 4 months after pFCI and then gradually returned to that of baseline at 8 months (preocclusion value: 83.6 mmHg ± 3.7 mmHg; 4 months value after MCAO: 95.4 mmHg ± 5.4 mmHg, $p^{*}<0.01$; 8 months after MCAO value: 87.4 mmHg ± 6.2 mmHg) (Figure 6A).

The body temperature and weight were also monitored at several time points after pFCI in daylight cycle (Figure 6B and 6C). The body temperature was significantly lower than that of sham-operation at all time points by 6 months after ischemic injury (within a week

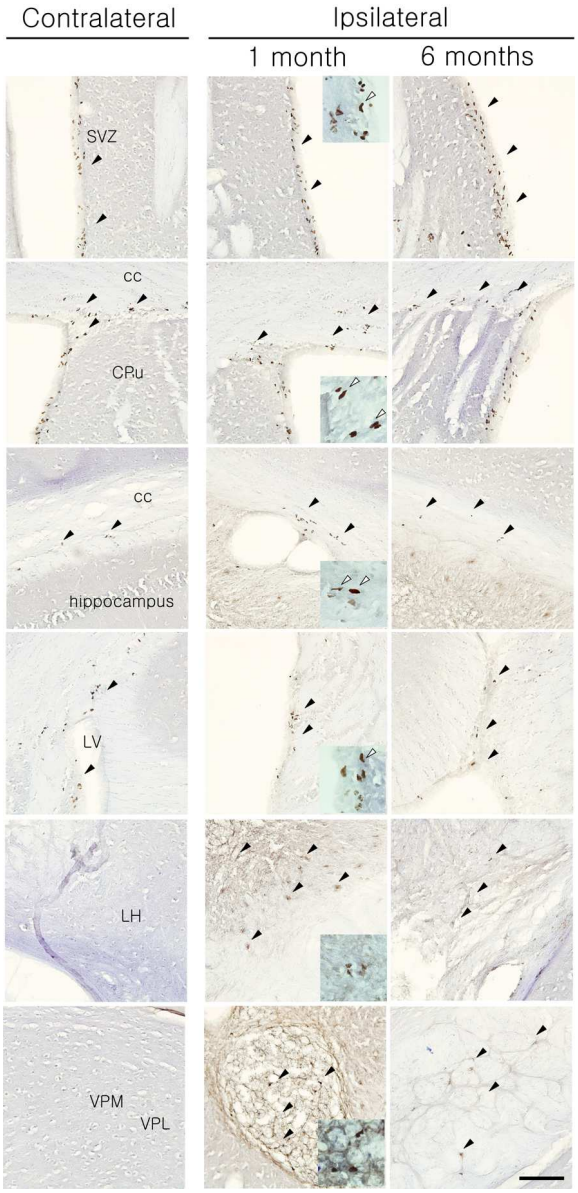

Figure 5. BrdU- immunostaining after pFCI. BrdU positive cells were detected in SVZ and corpus callosum in both hemisphere and increased in SVZ, thalamic and hypothalamic areas in ipsilateral side at 1 month and 6months. BrdU positive fugiform-shaped nuclei were also observed in SVZ, cc (white arrow). Scale bar = 100㎛.

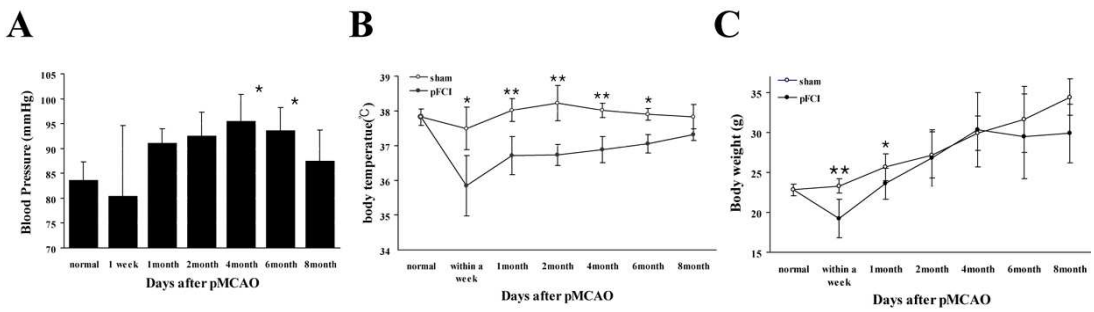

Figure 6. Evaluation of physiological recovery related anatomical reorganization. Temporally, a significant improvement in (A) blood pressure, (B) body temperature, and (C) Body weight were observed after excessive functional failure with ischemic injury. This improvement was shown especially from 6 months after pFCI and physiological functions were returned to normal level nearly at 8 months.

after sham-operation: 37.5℃ ± 0.6℃, after pFCI: 35.8℃ ± 0.9℃, p*=0.002; 1month-sham: 38.0℃ ± 0.3℃, -pFCI: 36.7℃ ± 0.6℃, p**<0.001; 2 months-sham: 38.2℃ ± 0.5℃, -pFCI: 36.7℃ ± 0.3℃, p**<0.001 ; 4 months-sham: 38.0℃± 0.2℃, -pFCI: 36.9℃ ± 0.4℃, p**<0.001 ; 6 months-sham: 37.9℃ ± 0.2℃, -pFCI: 37.1℃ ± 0.3℃, p*=0.003). However it also returned close that of the baseline sham-operation value at 8 months (8 months-sham: 37.8℃ ± 0.4℃, -pFCI: 37.3℃ ± 0.2℃). The mean weight of pFCI groups was shown also to recover gradually in time-dependent manner. At the first 1month after ischemic injury, the mean weight of pFCI groups was significantly lower than that of sham-operation groups (within a week-sham: 23.3g ± 0.9g, -pFCI: 19.2g ± 2.4g, p**<0.001; 1month-sham: 25.7g ± 1.7g, -pFCI: 23.6g ± 1.9g, p*=0.004), which was returned nearly to the sham-operation value at 2 months. Thereafter it had reduced again and stabilized at the significantly lower value until 8months (8 months-sham: 34.5g ± 2.3g, -MCAO: 29.9g ± 3.6g, p**<0.001).

7. Elevated plus maze test

To assess the role of NA in anxiety-like behavior, mice were subjected to elevated plus maze tests at several time points after pFCI (Table 2). At 2 months after pFCI, mice spent a significantly more time on the open arms of the plus maze than sham-operated mice and the number of open arms entry was also higher in pFCI mice than sham-operated mice, which were returned to that of control mice by 6month after pFCI. The number of closed arms entry and the time stayed on the closed arms were not significant different. These

Table 2. Summary of behavioral measures on the elevated plus-maze following pFCI

behavioral data	Within a week		1 month		2 months		4months		6 months	
	sham	pFCI	sham	pFCI	sham	pFCI	sham	pFCI	sham	pFCI
Time spent in open arms (s)	2.2±1.5	11.0±2.3**	7.6±2.9	14.7±4.0*	10.4±2.4	14.9±3.2*	12.0±3.7	9.7±5.6	5.3±1.0	8.6±4.8
Time spent in closed arms (s)	51.4±5.0	30.0±9.5*	31.2±8.7	26.8±8.0	36.6±8.9	29.6±7.1	32.3±3.4	36.3±8.8	26.3±8.7	37.4±6.7*
Number of open arm entries (times)	1.0±0.7	0.3±0.6	1.6±0.9	1.4±1.1	1.2±0.8	1.2±1.1	2.5±0.6	1.8±1.0	1.8±0.5	2.7±1.1
Number of closed arm entries (times)	2.4±1.5	1.3±0.6	2.6±0.9	2.2±1.3	2.2±0.4	2.4±0.9	3.3±1.3	3.3±1.0	3.3±1.5	3.1±1.5

Values are mean ± STD. Significant difference from sham group by student' *t*-test, **P*<0.05, ***P*<0.001.

data suggested that pFCI conferred anxiolytic effects to mice initially but gradually dissipated over time upon the recovery of neurological deficits and the reorganization of NA circuitry.

IV. DISCUSSION

This study demonstrated the feasibility of transsynaptic labeling by using WGA-expressing adenoviral vector in the mouse noradrenergic system. By simply injecting the virus solution into the unilateral LC, the noradrenergic neural pathways were clearly visualized with great accuracy and high reproducibility from LC to its projectional areas in this study (Figure 2). An early work using horseradish peroxidase in rat[39] demonstrated a topographic organization within the LC nucleus such that cells projecting to hippocampus and septum were located in the dorsal LC, those projecting to cerebellum were in both dorsal and ventral LC, and those projecting to the thalamus and hypothalamus were in the caudal and rostral poles. Later work showed that cortically- projecting LC neurons were more prominent within the caudal portion of nucleus and these neurons projected in a predominantly ipsilateral (>95%) manner.[40] In contrast to this previous study, symmetric bilateral projections to both hemispheres were shown in this study. Recently, the tracing study of olfactory system by using coexpression of barley lectin gene and odorant receptor gene revealed symmetric bilateral projections from olfactory epithelium to olfactory center.[33]

Compared to the conventional method in which WGA protein was injected into target sites, present method successfully and reliably detected more strong transsynaptically transferred WGA protein, which might be related to efficient infection of adenovirus to the noradrenergic neurons as well as promoter elements (PRS promoter) being used for robust expression of WGA. PRS has previously been shown to be an NA-specific *cis* element binding to paired-like homeodomain factor Phox2a/Phox2b.[41, 42] It has been confirmed that

increasing copies of PRS cause synergistic activation of reporter gene expression reaching maximal efficacy at eight copies. An adenoviral construct containing eight copies of PRS was shown to induce strong expression of β-galactosidase in NA neurons upon its microinjection to LC,[38] which was in agreement with successful visualization of NA system in mouse brain with recombinant adenoviral vector expressing WGA under the control of PRS promoter elements in this study (Figure 1). Moreover, in higher magnification field, the observation of perikarya in remote areas from LC indicates that WGA protein underwent the anterograde transsynaptic transfer from LC. It was previously reported that WGA proteins appear in granule-like structures in neurons, bind to N-acetylglucosamine and sialic acid in carbohydrate moiety of glycoproteins and glycolipids expressed on neuronal surface plasma membrane, are efficiently taken up into neurons by endocytosis, and are transported through axons and dendrites.[26, 43] Similar appearance of WGA in neurons in the present study suggests that, following the synthesis and maturation in LC, WGA transgene product underwent the same endocytotic, secretory, and transfer pathways.

It has also successfully demonstrated the process of reorganization of NA circuitries after pFCI in a time-dependent manner in the present study. Intense WGA immunoreactivity was initially detected in the contralateral side and the ipsilateral non-lesioned areas, which was followed by subsequent appearance in several areas of infarction by pFCI, such as thalamic nucleus, lateral hypothalamic area, lateral habenular nucleus, and amygdala. These findings suggest that compensatory reinforcement of undamaged ipsilateral sites and contralateral NA circuits occurred shortly after the onset of pFCI and

then evolved into subsequent reorganization of NA circuitries in severely damaged area. The recovery and reorganization of neural circuitries in the lesion may be mediated by compensatory sproutings of neuronal processes in intact areas as well as novel endogenous repair strategy in injured spinal cord of adult rat.[44, 45, 35] Recently, a comprehensive review of data obtained from PET, fMRI and transcranial magnetic stimulation methods supports the general hypothesis that clinical recovery after a stroke is associated with increased neuronal activities in non-injured brain areas.[46, 47] In this study, it was interesting to find strong WGA immunoreactivity never seen in non-injured mice in the hippocampal fissure and SVZ at the edge of damaged hippocampus, which was not seen in non-injured mice after pFCI (Figure 4, black arrow). It has been found that an acute stroke induced by MCAO precipitates cellular proliferation or neurogenesis in the ipsilateral SVZ and a large number of immature neurons migrate from SVZ to ipsilateral infracted areas.[48-50] Previous studies showed a large number of migrating neuroblasts extending from the SVZ laterally up to the ischemic lesion in a gradient at 2 weeks following insults.[48, 50] The strong WGA immunoreactivity in the hippocampus and adjacent SVZ in present study may represent those newly proliferated, migrating neurons executing a crucial role in the recovery of damaged area after pFCI. To confirm this hypothesis, BrdU immunohistochemistry, a thymidine analogue, was used at 1month and 6month after pFCI (Figure 5). BrdU is incorporated into the proliferating cell nuclei during the S-phase of a cell cycle for DNA duplication and has been widely used to explore neural stem cell proliferation in the central nervous system.[51, 52] It was also known that brain insults such as cerebral ischemia and epileptic seizures, causing neuronal death, are accompanied by increased neurogenesis in

the SGZ and SVZ.[53, 54] BrdU positive cells were observed in thalamic and hypothalamic lesions, increased BrdU positive cells in SVZ, and fusiform-shaped nuclei in SVZ and corpus callosum, which was consistent with the process of initial neuronal proliferation in SVZ and their subsequent migration into the ischemic lesions as a repair mechanism.

To assess the relationship of remodeling process with functional recovery in NA system, the alteration of blood pressure, body temperature, weight, and behavior was investigated on several time points after pFCI (figure 6). In this study, data showed that the gradual recovery of blood pressure, body temperature, body weight, and behavior following acute infarction was closely related with the anatomical reorganization of hypothalamus, thalamus, and amygdala at 6month of pFCI. Dysfunction of the NA system has been widely known to be associated with alterations of blood pressure[8, 56-58], body temperature[59-61] and weight[62], and anxiety.[9, 63] Previous experiments indicated that blood pressure was significantly higher in mice having insular infarction.[8, 57] Insular cortex is directly connected with central nucleus of the amygdala, the posterior lateral hypothalamus, and the parabrachial nucleus[64-66] belonging to NA system. Although WGA immunoreactivity was not detected in the insular cortex in this study, it was speculated that the lateral hypothalamus, amygdala, and parabrachial nucleus are directly connected with insular cortex and the circuitry damage is responsible for the dysfunction and recovery of blood pressure. Early studies also found that lesions of hypothalamic nucleus or thalamic nucleus resulted in alterations of body temperature and body weight in models of MPTP-neurotoxicity in pFCI, ischemic injury, and stereotaxic injury.[60, 61, 67] In line with these studies, the present results seem to explain that the altered physiological dysfunction

precipitated by acute insults in above anatomical structures may gradually recover as the reorganization processes of damaged NA systems mature in those structures. As shown in table 2, using the elevated plus maze, significant reduction was found in anxiety-like behavior in a time-dependent manner with the anatomical changes following pFCI, as displayed by an increase in time spent on the open arms. The locomotor activity of animals, represented by the number of closed arms entries, was not significantly different between sham-operation and pFCI group. Therefore, a decrease in anxiety is independent of any changes in locomotor activity. Increase in NA signaling is associated with hightened anxiety and decrease in NA signaling is related with less anxiety. Central administration of adrenergic antagonists or lesions of the locus coeruleus in rats reduced anxiogenic effects in the elevated plus maze.[68, 69] The results of present study are again in agreement with initial dysfunction of NA activities and following its gradual recovery over time along with reorganization of NA circuits in the infracted structures.

In conclusion, the results were successfully visualized the circuitries of noradrenergic system in mice by using transsynaptic tracing with PRS-WGA adenovirus and confirmed the phenomenon of reorganization of damaged NA circuitries before and after pFCI. Moreover, there were close temporal relationships between the physiological and functional recovery and the reorganization of damaged NA circuits. The process of reorganization may involve axonal sprouting of intact NA projections making synapses on newly proliferated and migrated neurons to the infarct area, which require further clarification by additional studies.

V. CONCLUSION

This study successfully visualized transsynaptic labeling by using the WGA-expressing adenoviral vector in the mouse noradrenergic system. This may be due to the efficient infection of adenovirus to the NA neurons and to the PRS promoter inducing robust expression of WGA. It was also confirmed that damaged noradrenergic circuitry was reformed and remodeled pFCI model. The importance of the remodeling of NA circuitry in the damaged area for functional recovery was also evaluated by monitoring blood pressure, body temperature and weight, and behavior in several time points, which were nicely correlated. The results were elucidated that anatomical alteration of NA system correlated to the functional recovery in a mouse stroke model. Therefore, this study supported that anatomical neural plasticity contributes to functional recovery in noradrenergic system in adult mice.

In addition, this study has provided evidence that the WGA-expressing adenoviral vector system using cell-type specific promoter is an extremely valuable tool for the investigations of formation, refinement, maintenance, and remodeling of neural networks as well as their functional implications.

IV. REFERENCE

1. Silver FL, Norris JW, Lewis AJ, Hachinski VC. Early mortality following stroke: a prospective review. *Stroke.* May-Jun 1984;15(3):492-496.

2. Myers MG, Norris JW, Hachniski VC, Sole MJ. Plasma norepinephrine in stroke. *Stroke.* Mar-Apr 1981;12(2):200-204.

3. Norris JW, Froggatt GM, Hachinski VC. Cardiac arrhythmias in acute stroke. *Stroke.* Jul-Aug 1978;9(4):392-396.

4. Norris JW, Hachinski VC, Myers MG, Callow J, Wong T, Moore RW. Serum cardiac enzymes in stroke. *Stroke.* Sep-Oct 1979;10(5):548-553.

5. Tokgozoglu SL, Batur MK, Top uoglu MA, Saribas O, Kes S, Oto A. Effects of stroke localization on cardiac autonomic balance and sudden death. *Stroke.* Jul 1999;30(7):1307-1311.

6. Wang TD, Wu CC, Lee YT. Myocardial stunning after cerebral infarction. *Int J Cardiol.* Feb 1997;58(3):308-311.

7. Bloomfield SA, Jackson RD, Mysiw WJ. Catecholamine response to exercise and training in individuals with spinal cord injury. *Med Sci Sports Exerc.* Oct 1994;26(10):1213-1219.

8. Smith KE, Hachinski VC, Gibson CJ, Ciriello J. Changes in plasma catecholamine levels after insula damage in experimental stroke. *Brain Res.* Jun 4 1986;375(1):182-185.

9. Marino MD, Bourdelat-Parks BN, Cameron Liles L, Weinshenker D. Genetic reduction of noradrenergic function alters social memory and reduces aggression in mice. *Behav Brain Res.* Jun 20 2005;161(2):197-203.

10. Cecchi M, Khoshbouei H, Morilak DA. Modulatory effects of norepinephrine, acting on alpha 1 receptors in the central nucleus of the amygdala, on behavioral and neuroendocrine responses to acute immobilization stress. *Neuropharmacology.* Dec 2002;43(7):1139-1147.

11. Marcin MS, Nemeroff CB. The neurobiology of social anxiety disorder: the relevance of fear and anxiety. *Acta Psychiatr Scand Suppl.* 2003(417):51-64.

12. Sander D, Winbeck K, Klingelhofer J, Etgen T, Conrad B. Prognostic relevance of pathological sympathetic activation after acute thromboembolic stroke. *Neurology.*

Sep 11 2001;57(5):833-838.

13. Cechetto DF, Chen SJ. Subcortical sites mediating sympathetic responses from insular cortex in rats. *Am J Physiol.* Jan 1990;258(1 Pt 2):R245-255.

14. Cechetto DF. Identification of a cortical site for stress-induced cardiovascular dysfunction. *Integr Physiol Behav Sci.* Oct-Dec 1994;29(4):362-373.

15. Hallett M. Plasticity of the human motor cortex and recovery from stroke. *Brain Res Brain Res Rev.* Oct 2001;36(2-3):169-174.

16. Rijntjes M, Weiller C. Recovery of motor and language abilities after stroke: the contribution of functional imaging. *Prog Neurobiol.* Feb 2002;66(2):109-122.

17. Reinecke S, Lutzenburg M, Hagemann G, Bruehl C, Neumann-Haefelin T, Witte OW. Electrophysiological transcortical diaschisis after middle cerebral artery occlusion (MCAO) in rats. *Neurosci Lett.* Feb 12 1999;261(1-2):85-88.

18. Que M, Schiene K, Witte OW, Zilles K. Widespread up-regulation of N-methyl-D-aspartate receptors after focal photothrombotic lesion in rat brain. *Neurosci Lett.* Oct 1 1999;273(2):77-80.

19. Buchkremer-Ratzmann I, August M, Hagemann G, Witte OW. Electrophysiological transcortical diaschisis after cortical photothrombosis in rat brain. *Stroke.* Jun 1996;27(6):1105-1109; discussion 1109-1111.

20. Yoshihara Y, Mizuno T, Nakahira M, et al. A genetic approach to visualization of multisynaptic neural pathways using plant lectin transgene. *Neuron.* Jan 1999;22(1):33-41.

21. Yoshihara Y. Visualizing selective neural pathways with WGA transgene: combination of neuroanatomy with gene technology. *Neurosci Res.* Oct 2002;44(2):133-140.

22. Kinoshita N, Mizuno T, Yoshihara Y. Adenovirus-mediated WGA gene delivery for transsynaptic labeling of mouse olfactory pathways. *Chem Senses.* Mar 2002;27(3):215-223.

23. Gonatas NK, Harper C, Mizutani T, Gonatas JO. Superior sensitivity of conjugates of horseradish peroxidase with wheat germ agglutinin for studies of retrograde axonal transport. *J Histochem Cytochem.* Mar 1979;27(3):728-734.

24. Itaya SK. Anterograde transsynaptic transport of WGA-HRP in rat olfactory pathways. *Brain Res.* Apr 21 1987;409(2):205-214.

25. Burright EN, Clark HB, Servadio A, et al. SCA1 transgenic mice: a model for neurodegeneration caused by an expanded CAG trinucleotide repeat. *Cell.* Sep 22 1995;82(6):937-948.

26. Fabian RH, Coulter JD. Transneuronal transport of lectins. *Brain Res.* Sep 30 1985;344(1):41-48.

27. Itaya SK, van Hoesen GW. WGA-HRP as a transneuronal marker in the visual pathways of monkey and rat. *Brain Res.* Mar 18 1982;236(1):199-204.

28. Ruda M, Coulter JD. Axonal and transneuronal transport of wheat germ agglutinin demonstrated by immunocytochemistry. *Brain Res.* Oct 14 1982;249(2):237-246.

29. Shipley MT. Transport of molecules from nose to brain: transneuronal anterograde and retrograde labeling in the rat olfactory system by wheat germ agglutinin-horseradish peroxidase applied to the nasal epithelium. *Brain Res Bull.* Aug 1985;15(2):129-142.

30. Lee HS, Kim MA, Waterhouse BD. Retrograde double-labeling study of common afferent projections to the dorsal raphe and the nuclear core of the locus coeruleus in the rat. *J Comp Neurol.* Jan 10 2005;481(2):179-193.

31. Byrum CE, Guyenet PG. Afferent and efferent connections of the A5 noradrenergic cell group in the rat. *J Comp Neurol.* Jul 22 1987;261(4):529-542.

32. Hanno Y, Nakahira M, Jishage K, Noda T, Yoshihara Y. Tracking mouse visual pathways with WGA transgene. *Eur J Neurosci.* Nov 2003;18(10):2910-2914.

33. Zou Z, Horowitz LF, Montmayeur JP, Snapper S, Buck LB. Genetic tracing reveals a stereotyped sensory map in the olfactory cortex. *Nature.* Nov 8 2001;414(6860):173-179.

34. Sugita M, Shiba Y. Genetic tracing shows segregation of taste neuronal circuitries for bitter and sweet. *Science.* Jul 29 2005;309(5735):781-785.

35. Bareyre FM, Kerschensteiner M, Raineteau O, Mettenleiter TC, Weinmann O, Schwab ME. The injured spinal cord spontaneously forms a new intraspinal circuit in adult rats. *Nat Neurosci.* Mar 2004;7(3):269-277.

36. Vakili A, Kataoka H, Plesnila N. Role of arginine vasopressin V1 and V2 receptors for brain damage after transient focal cerebral ischemia. *J Cereb Blood Flow Metab.* Aug 2005;25(8):1012-1019.

37. Huang Z, Huang PL, Panahian N, Dalkara T, Fishman MC, Moskowitz MA.

Effects of cerebral ischemia in mice deficient in neuronal nitric oxide synthase. *Science.* Sep 23 1994;265(5180):1883-1885.

38. Hwang DY, Carlezon WA, Jr., Isacson O, Kim KS. A high-efficiency synthetic promoter that drives transgene expression selectively in noradrenergic neurons. *Hum Gene Ther.* Sep 20 2001;12(14):1731-1740.

39. Mason ST, Fibiger HC. Regional topography within noradrenergic locus coeruleus as revealed by retrograde transport of horseradish peroxidase. *J Comp Neurol.* Oct 15 1979;187(4):703-724.

40. Waterhouse BD, Lin CS, Burne RA, Woodward DJ. The distribution of neocortical projection neurons in the locus coeruleus. *J Comp Neurol.* Jul 10 1983;217(4):418-431.

41. Kim HS, Seo H, Yang C, Brunet JF, Kim KS. Noradrenergic-specific transcription of the dopamine beta-hydroxylase gene requires synergy of multiple cis-acting elements including at least two Phox2a-binding sites. *J Neurosci.* Oct 15 1998;18(20):8247-8260.

42. Yang C, Kim HS, Seo H, Kim CH, Brunet JF, Kim KS. Paired-like homeodomain proteins, Phox2a and Phox2b, are responsible for noradrenergic cell-specific transcription of the dopamine beta-hydroxylase gene. *J Neurochem.* Nov 1998;71(5):1813-1826.

43. Broadwell RD, Balin BJ. Endocytic and exocytic pathways of the neuronal secretory process and trans-synaptic transfer of wheat germ agglutinin-horseradish peroxidase in vivo. *J Comp Neurol.* Dec 22 1985;242(4):632-650.

44. Raineteau O, Fouad K, Noth P, Thallmair M, Schwab ME. Functional switch between motor tracts in the presence of the mAb IN-1 in the adult rat. *Proc Natl Acad Sci U S A.* Jun 5 2001;98(12):6929-6934.

45. Bareyre FM, Haudenschild B, Schwab ME. Long-lasting sprouting and gene expression changes induced by the monoclonal antibody IN-1 in the adult spinal cord. *J Neurosci.* Aug 15 2002;22(16):7097-7110.

46. Rossini PM, Calautti C, Pauri F, Baron JC. Post-stroke plastic reorganisation in the adult brain. *Lancet Neurol.* Aug 2003;2(8):493-502.

47. Calabresi P, Centonze D, Pisani A, Cupini L, Bernardi G. Synaptic plasticity in the ischaemic brain. *Lancet Neurol.* Oct 2003;2(10):622-629.

48. Arvidsson A, Collin T, Kirik D, Kokaia Z, Lindvall O. Neuronal replacement from endogenous precursors in the adult brain after stroke. *Nat Med.* Sep 2002;8(9):963-970.

49. Parent JM, Vexler ZS, Gong C, Derugin N, Ferriero DM. Rat forebrain neurogenesis and striatal neuron replacement after focal stroke. *Ann Neurol.* Dec 2002;52(6):802-813.

50. Kokaia Z, Lindvall O. Neurogenesis after ischaemic brain insults. *Curr Opin Neurobiol.* Feb 2003;13(1):127-132.

51. Reynolds BA, Weiss S. Generation of neurons and astrocytes from isolated cells of the adult mammalian central nervous system. *Science.* Mar 27 1992;255(5052):1707-1710.

52. Miller MW, Nowakowski RS. Use of bromodeoxyuridine-immunohistochemistry to examine the proliferation, migration and time of origin of cells in the central nervous system. *Brain Res.* Aug 2 1988;457(1):44-52.

53. Jin K, Minami M, Lan JQ, et al. Neurogenesis in dentate subgranular zone and rostral subventricular zone after focal cerebral ischemia in the rat. *Proc Natl Acad Sci U S A.* Apr 10 2001;98(8):4710-4715.

54. Zhang RL, Zhang ZG, Zhang L, Chopp M. Proliferation and differentiation of progenitor cells in the cortex and the subventricular zone in the adult rat after focal cerebral ischemia. *Neuroscience.* 2001;105(1):33-41.

55. Jiang W, Gu W, Brannstrom T, Rosqvist R, Wester P. Cortical neurogenesis in adult rats after transient middle cerebral artery occlusion. *Stroke.* May 2001;32(5):1201-1207.

56. Lambert GW. Paring down on Descartes: a review of brain noradrenaline and sympathetic nervous function. *Clin Exp Pharmacol Physiol.* Dec 2001;28(12):979-982.

57. Meyer S, Strittmatter M, Fischer C, Georg T, Schmitz B. Lateralization in autonomic dysfunction in ischemic stroke involving the insular cortex. *Neuroreport.* Feb 9 2004;15(2):357-361.

58. Schmid A, Huonker M, Barturen JM, et al. Catecholamines, heart rate, and oxygen uptake during exercise in persons with spinal cord injury. *J Appl Physiol.* Aug 1998;85(2):635-641.

59. Ali SF, Newport GD, Slikker W, Jr. Methamphetamine-induced dopaminergic toxicity in mice. Role of environmental temperature and pharmacological agents. *Ann N Y Acad Sci.* Oct 31 1996;801:187-198.

60. Corbett D, Thornhill J. Temperature modulation (hypothermic and hyperthermic conditions) and its influence on histological and behavioral outcomes following cerebral ischemia. *Brain Pathol.* Jan 2000;10(1):145-152.

61. Moy LY, Albers DS, Sonsalla PK. Lowering ambient or core body temperature elevates striatal MPP+ levels and enhances toxicity to dopamine neurons in MPTP-treated mice. *Brain Res.* Apr 20 1998;790(1-2):264-269.

62. King BM. The rise, fall, and resurrection of the ventromedial hypothalamus in the regulation of feeding behavior and body weight. *Physiol Behav.* Feb 28 2006;87(2):221-244.

63. Pandaranandaka J, Poonyachoti S, Kalandakanond-Thongsong S. Anxiolytic property of estrogen related to the changes of the monoamine levels in various brain regions of ovariectomized rats. *Physiol Behav.* Apr 15 2006;87(4):828-835.

64. Mufson EJ, Mesulam MM, Pandya DN. Insular interconnections with the amygdala in the rhesus monkey. *Neuroscience.* 1981;6(7):1231-1248.

65. Saper CB. Convergence of autonomic and limbic connections in the insular cortex of the rat. *J Comp Neurol.* Sep 10 1982;210(2):163-173.

66. Shipley MT, Sanders MS. Special senses are really special: evidence for a reciprocal, bilateral pathway between insular cortex and nucleus parabrachialis. *Brain Res Bull.* May 1982;8(5):493-501.

67. Marien MR, Colpaert FC, Rosenquist AC. Noradrenergic mechanisms in neurodegenerative diseases: a theory. *Brain Res Brain Res Rev.* Apr 2004;45(1):38-78.

68. Cecchi M, Khoshbouei H, Javors M, Morilak DA. Modulatory effects of norepinephrine in the lateral bed nucleus of the stria terminalis on behavioral and neuroendocrine responses to acute stress. *Neuroscience.* 2002;112(1):13-21.

69. Lapiz MD, Mateo Y, Durkin S, Parker T, Marsden CA. Effects of central noradrenaline depletion by the selective neurotoxin DSP-4 on the behaviour of the isolated rat in the elevated plus maze and water maze. *Psychopharmacology (Berl).* May 2001;155(3):251-259.

ABSTRACT (IN KOREAN)

영구적 국소 대뇌 허혈 모델에서 유전학적 추적기법을 이용한 노르에피네프린성 청색반점 뇌신경 연결로의 변화 및 가소성 규명

<지도교수 이 병 인>

연세대학교 대학원 의과학과

김 현 정

뇌의 다양한 기능적인 측면을 연구하기 위해서는 뇌신경 연결과 그 가소성(plasticity)에 대한 자세한 정보가 없어서는 안 된다. 특정 promoter의 조절 하에 WGA의 cDNA를 발현시키는 유전학적 방법이 선택적이고 기능적인 뇌신경 회로의 시각화를 위해 새롭게 도입되었다. 급성 뇌허혈에서 뿐만 아니라 알츠하이머병 및 파킨슨병 등과 같은 여러 신경퇴행성 질환과 노르에피네프린성 신경계의 기능장애와의 연관성에 대해서는 이미 널리 보고된 바 있다. 그러나 대뇌 허혈의 급성 및 만성 회복기에 노르에피네프린성 뇌신경망의 손상 부위 및 범위와 기능적인 연관성에 대해서는 아직 명확하게 밝혀진 바가 없다. 이러한 배경 하에, 본 연구에서는 새로운 유전학적 추적 기법을 이용하여 노르에피네프린성 신경회로망의 시각화를 시도하였다. 더불어 영구적 국소 대뇌 허혈 유도 후, 노르에피네프린성 신경회로망의 구조적 손상과 이후 이어지는 변화 및 이에 대한 기능적인 연관성에 대해서도 조사하였다.

수컷 C57BL/6 마우스에서 중대뇌동맥을 폐색함으로써 영구적 국소 대뇌 허혈 모델을 만들어 실험에 이용하였으며, 국부적 대뇌 혈류 및 혈압을 측정하였

다. 노르에피네프린성 신경세포에 특이적인 PRS promoter의 조절 하에 WGA cDNA를 도입한 recombinant adenoviral vector를 마우스의 대뇌 허혈을 일으킨 대뇌반구 측의 LC에 주입하였다. 면역화학염색과 *in situ* hybridization 기법을 이용하여 대조군 및 대뇌 허혈 유도군에서 WGA 단백질 및 mRNA의 발현 양상을 관찰하였다. 새로운 신경세포의 형성 및 재생 과정의 관찰을 위하여 BrdU 면역염색을 시행하였다. 또한 혈압, 체온 및 체중과 불안증 관련 행동검사도 수행하였다.

정상적인 뇌에서는 강한 WGA 면역활성이 pontine reticular nucleus, thalamic nucleus, lateral hypothalamic area, amygdala 및 olfactory bulb 등의 뇌 광범위한 부분에서 발현되어 있음을 관찰하였다. 또한 대뇌 허혈 유도 전과 후의 transsynaptic tracing 및 BrdU 면역염색을 통해 손상되었던 노르에피네프린성 뇌신경회로가 재형성되고 개조되는 현상을 관찰하였고, 특히 thalamic nucleus, lateral hypothalamic area, and amygdale등의 몇몇 특정 부분의 재구성과 더불어 기능적인 회복이 일어났음을 확인하였다.

결론적으로, 이번 연구에서는 마우스 성체의 노르에피네프린성 신경계에서 구조적 신경 가소성이 기능적인 회복에 기여함을 확인할 수 있었다.

핵심 되는 말: 국소 대뇌 허혈; 노르에피네프린; Agglutinins, Wheat Germ; Vector, Genetic; 신경가소성